ELSEVIER

Earth and Planetary Science Letters 209 (2003) 245–255

EPSL

www.elsevier.com/locate/epsl

The effect of pressure on partitioning of Ni and Co between silicate and iron-rich metal liquids: a diamond-anvil cell study

M. Ali Bouhifd [1], Andrew P. Jephcoat *

Department of Earth Sciences, University of Oxford, Parks Road, Oxford OX1 3PR, UK

Received 7 August 2002; received in revised form 6 November 2002; accepted 5 February 2003

Abstract

High-pressure and high-temperature experiments have been conducted with a laser-heated diamond-anvil cell (LHDAC) to determine the partition coefficients for Ni and Co up to 42 GPa and around 2500 K. Comparison of the present experimental data with those of multi-anvil devices shows a good agreement between the different exchange partitioning coefficients. The agreement suggests conditions in LHDAC experiments can reproduce those of multi-anvil experiments in the pressure range studied. Up to the maximum pressure reached in our work, Ni and Co become less siderophile with increasing pressure, as already observed in previous studies at lower pressures. Our data, combined with lower-pressure results, suggest a magma ocean would have extended to as much as 45 GPa (near 1200 km in depth) in order to obtain homogeneous equilibrium between core-forming metals and the silicate mantle in the early Earth.

Keywords: Earth's core formation; laser-heated diamond-anvil cell; high-pressure; magma ocean; metal–silicate segregation; siderophile elements

1. Introduction

It is very well known that the main feature of the Earth is its differentiation into a iron-rich core and a silicate mantle. As a result of core formation, the Earth's mantle is depleted in siderophile elements, but the pattern of this depletion cannot be explained by simple metal–silicate segregation at low pressures [1–5] (see Walter et al. [6] for a review). This poor agreement between the calculated depletions based on low-pressure metal–silicate partition coefficients and the observed depletions was the basis of an argument for heterogeneous accretion scenarios in which the mantle did not equilibrate with iron-rich metal [3,4,7]. At the same time, other scenarios have been proposed to account for this apparent disequilibrium, including inefficient core formation [8,9] or equilibration at high pressure and high temperature at the base of a magma ocean [10–12]. In this context, the behaviour of Ni and Co has been considered to provide an important clue, both being

* Corresponding author. Tel.: +44-1865-272067; Fax: +44-1865-272072.
E-mail address: andrew@earth.ox.ac.uk (A.P. Jephcoat).

[1] Present address: IPGP, Laboratoire des Géomatériaux, 4 Place Jussieu, 75252 Paris Cedex 05, France.

0012-821X/03/$ – see front matter
doi:10.1016/S0012-821X(03)00076-1

refractory elements and present in the mantle in a near-chondritic Ni to Co ratio [13]. In addition, Ni and Co are almost identical to Fe in cosmochemical volatility [14,15]. The partitioning of Ni and Co has been studied up to 26 GPa by many authors: Hillgren et al. [16] studied partitioning of Fe, Ni and Co in the iron–basaltic silicate system at 10 GPa and 2000°C and showed a decrease in the partitioning coefficients for Ni and Co, compared to values at 1 atm and 1260°C. Thibault and Walter [17] investigated the molten iron/silicate liquid partitioning of Ni and Co in a model C1 chondrite at pressures of 1.2–12 GPa and temperatures of 2123–2750 K. They showed that both increasing pressure and temperature result in lowering the exchange partition coefficients of Ni and Co and that the pressure effect is significantly more important than the temperature effect for reasonable geotherms. Li and Agee [11,12] have performed a number of experiments to determine the partitioning of Ni and Co between S-bearing iron and silicate liquid. For a composition derived from the Allende meteorite up to 20 GPa and by extrapolating the partition coefficients to higher pressures, they concluded that the observed abundances of Ni and Co and the Ni to Co ratio in the mantle can be explained if core segregation took place in a magma ocean with a depth of 750–1100 km. The more recent [12] study with similar composition extended the depth required to between 1200 and 1450 km (43 and 59 GPa, 2400 and 4200 K).

In the present work we use the laser-heated diamond-anvil cell (LHDAC) to study the high-pressure and -temperature partitioning of Ni and Co between iron-rich metal and silicate liquids up to 42 GPa. Our first aim is to compare our partitioning behaviour of Ni and Co at low pressures (5–12 GPa) with results from multi-anvil devices in the Si–Al–Fe–Mg–Ca–Ni–Co–O system [17]. The success of these comparisons will substantially increase confidence in the extension of partitioning experiments to lower-mantle conditions. Only the effect of pressure up to 42 GPa has been studied in this work, other parameters affecting the partitioning of Ni and Co (the chemical composition of the silicate and metal liquids, oxygen fugacity, temperature) were kept constant – at least within the range of the uncertainty of the experiments. The logical next steps will be the extension of such studies to include a range of parameters affecting partitioning coefficients. We also discuss our results in the light of the different models proposed to explain core formation during early Earth differentiation.

2. Experimental techniques

2.1. Starting materials

Two starting compositions were used in this study and are listed in Table 1. They are similar to the compositions C1/C and C1/D used by Thibault and Walter [17]. Starting compositions consisted of a glass of C1 chondrite composition mixed with either iron and nickel or iron and cobalt metal powders. The bulk composition was prepared from oxide and carbonate mixes through repeated cycles of grinding and fusion at around 1800 K and rapidly cooled to obtain the glass of C1 chondrite used for the partitioning experiments. The appropriate amounts of Fe, Ni or Co were then added to separate mixes. Each composition was mixed and ground under ethanol, and finally dried at around 100°C for at least 24 h. We took great care to ensure that the grain size of particles in the starting materials did not exceed 3 μm. The proportions of SiO_2, Al_2O_3, MgO, CaO and Fe in both starting compositions were chosen to be that of model C1 chondrite.

Table 1
Composition of starting materials (wt%)[a]

	CNF[b]	CCF[c]
SiO_2	33.5	33.5
Al_2O_3	2.5	2.5
FeO	3.7	3.8
MgO	23.8	24.0
CaO	2.0	2.0
Fe	24.2	24.2
Ni	10.3	
Co		10.0

[a] Compositions similar to C1/C and C1/D of Thibault and Walter [17].
[b] CNF: Glass C1 chondrite+Ni and Fe metals.
[c] CCF: Glass C1 chondrite+Co and Fe metals.

Pure metal Ni and Co were added to the mixtures to make up ~10 wt% of the composition. As discussed by Thibault and Walter [17], these amounts are much higher than the abundances of these elements in C1 chondrite, and are required in order to obtain stable analyses of these elements with the electron microprobe. With such high concentrations of Ni and Co in the starting materials, it is possible that deviations from Henry's law might take place. After experiments, the concentration in the silicate liquid of NiO and CoO varied from 0.1 to 0.8 wt% and 0.5 to 0.9 wt%, respectively (Table 2a,b), where it is reasonable to consider that Henry's law applies [17].

2.2. High-pressure cell and samples

A typical sample configuration in the LHDAC is shown in Fig. 1. A hole drilled in the centre of the gasket constitutes the pressure chamber. For our high-pressure and high-temperature experiments, we used diamond anvils with 500 μm culets, and stainless-steel or Re gaskets preindented to a thickness of around 50 μm and drilled to a diameter of 100–150 μm (depending on the maximum pressure reached). Samples were mounted in the pressure chamber and dry argon loaded with a high-pressure gas-loading technique at 200 MPa [18]. Ar served as pressure-transmitting medium for all runs. It has a thermal conductivity low enough to ensure thermal insulation of the sample from the upper diamond. With this configuration and even if the samples touched the lower diamond initially, we found that we could heat the samples effectively with the laser. Nominal pressures were measured by the ruby fluorescence method [19] and the hydrostatic pressure scale. In our experiments, the fluorescence emission of one or two ruby grains at the edge of the gasket hole was systematically recorded at room temperature before and after heating for each run. No differences were observed on both pressures.

The samples were heated by a multimode Nd-YAG laser for an average of 10–15 min. The laser-heating system used in our partitioning experiments has already been described in detail along with the fitting procedure for temperature measurement [20]. To reduce the temperature gradient across the samples, a relatively broad, defocused beam (hot-spot size around 20 μm, with central temperature gradients of less than 20 K/μm) was used. With this temperature gradient, the maxi-

Table 2a
Electron microprobe analyses of Ni-bearing run products (wt%)[a]

P (GPa)	3.8	5.0	9.8	22.4	31.7	42.0
T (K)[b]	2420	2450	2500	2500	2620	2680
Silicate						
SiO_2	39.2 ± 1.5	40.6 ± 1.0	40.4 ± 2.0	47.3 ± 1.5	47.7 ± 2.0	46.0 ± 1.8
Al_2O_3	4.66 ± 1.2	3.59 ± 0.5	2.34 ± 0.6	3.29 ± 0.5	2.64 ± 1.0	2.64 ± 1.8
FeO	9.33 ± 1.0	9.65 ± 1.0	8.50 ± 0.7	9.16 ± 1.5	8.80 ± 1.2	8.70 ± 1.7
MgO	41.1 ± 2.8	43.9 ± 2.5	47.8 ± 2.8	36.8 ± 3.0	37.8 ± 2.5	39.9 ± 2.0
CaO	2.54 ± 1.3	2.0 ± 0.5	0.66 ± 0.20	2.98 ± 0.5	2.54 ± 1.1	1.93 ± 1.0
NiO	0.14 ± 0.03	0.20 ± 0.04	0.28 ± 0.06	0.41 ± 0.04	0.54 ± 0.05	0.76 ± 0.06
Metal						
Fe	73.3 ± 2.0	71.2 ± 2.0	72.0 ± 2.0	73.2 ± 2.5	78.6 ± 3.0	82.2 ± 2.4
Ni	26.7 ± 1.5	28.8 ± 1.0	28.0 ± 1.0	26.8 ± 1.0	21.4 ± 1.5	17.8 ± 2.0
$\log fO_2$	−2.1	−2.1	−2.2	−2.1	−2.2	−2.3
$K^{Ni}_{met/sil}$	22.8 ± 7.8	18.7 ± 6.0	11.4 ± 3.9	8.0 ± 2.2	4.4 ± 1.1	2.5 ± 0.8
D_{Ni}	243 ± 68	180 ± 45	127 ± 35	84 ± 11	51 ± 7	30 ± 5
D_{Fe}	10 ± 1.5	10 ± 1.5	11 ± 1	10 ± 2	11 ± 2	12 ± 3

$K^{Ni}_{met/sil}$ is the exchange partition coefficient for Ni (see text).
D_X is the partition coefficient between silicate and metal of the element X.
D_X = (wt% X in metal)/(wt% X in silicate).
[a] Analyses are normalised to 100%. A maximum of 0.2 wt% and 0.02 wt% Ar dissolved in the silicate and the metal liquid, respectively, at low pressures.
[b] Temperature uncertainty ±200 K.

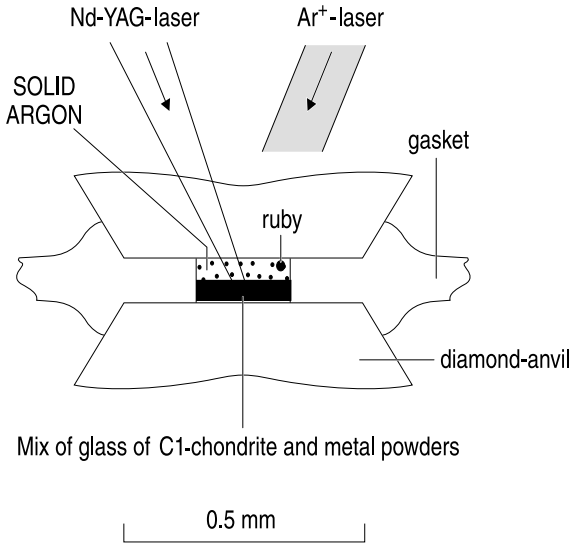

Fig. 1. A typical sample configuration in the LHDAC for partitioning experiments (see text for details).

mum difference between the temperatures at the centre and the edge of the laser spot is 200 K. Temperatures were determined spectro-radiometrically with a fit to a grey-body Planck function [20]. Great care was taken to scan the hot spot slowly over the whole sample, allowing each part of the sample chamber to be heated to the maximum temperature, forming uniform melt pools between silicate and metal. During this time, we collected one emission spectrum every 30 s and the temperature of the experiment is taken to be the mean of the temperatures derived from 20 or 30 emission spectra collected. In our experiments, we found that the difference between temperatures measured during one run did not exceed 100 K, but we have taken 200 K as a conservative uncertainty on the temperatures reported in Table 2a,b. An example of the thermal emission spectra collected during one run at 24 GPa is shown in Fig. 2. At higher pressures, we found that the silicate phase at 42 GPa melted at around 2700 ± 200 K, which is in reasonable agreement with the liquidus temperature at 40 GPa for C1 composition of about 3000 K determined by Miller et al. [21]. In our configuration it is impossible to quantify effects of the thermal pressure, but an increase of a few GPa on top of the nominal pressures reported was deduced by Andrault et al. [22].

2.3. Analytical technique

The small size of the diamond-anvil cell samples makes their chemical analysis challenging. In the first attempts to prepare DAC samples for chemical analysis, we embedded the recovered gasket in epoxy and polished the whole down to the heated surface, but with this technique a high percentage was lost. We found that our DAC samples can be directly analysed without any polishing, by taking care that the samples are welded to the edge of the gasket (without chemical inter-

Table 2b
Electron microprobe analyses of Co-bearing run products (wt%)

P (GPa)	2.7	5.2	9.9	24.4
T (K)	2515	2500	2520	2550
Silicate				
SiO_2	39.8 ± 2.0	40.4 ± 1.0	32.9 ± 2.0	39.2 ± 1.5
Al_2O_3	2.88 ± 1.5	1.05 ± 0.5	6.34 ± 0.6	4.29 ± 0.5
FeO	9.11 ± 1.0	7.96 ± 1.0	9.14 ± 0.7	7.28 ± 1.5
MgO	46.0 ± 3.0	49.2 ± 2.5	49.1 ± 2.8	46.5 ± 3.0
CaO	1.73 ± 0.7	0.86 ± 0.5	1.87 ± 0.20	1.79 ± 0.5
CoO	0.48 ± 0.06	0.56 ± 0.04	0.65 ± 0.06	0.94 ± 0.04
Metal				
Fe	76.5 ± 2.0	70.8 ± 2.0	69.7 ± 2.0	70.8 ± 2.5
Co	23.5 ± 1.5	29.2 ± 1.0	30.3 ± 1.0	29.2 ± 1.0
$\log fO_2$	−2.2	−2.2	−2.1	−2.3
$K^{Co}_{met/sil}$	5.8 ± 1.5	5.8 ± 1.3	6.0 ± 1.1	3.2 ± 1
D_{Co}	62 ± 11	66 ± 6	59 ± 7	39 ± 2.5
D_{Fe}	11 ± 1.6	11 ± 1.8	10 ± 1	12 ± 3

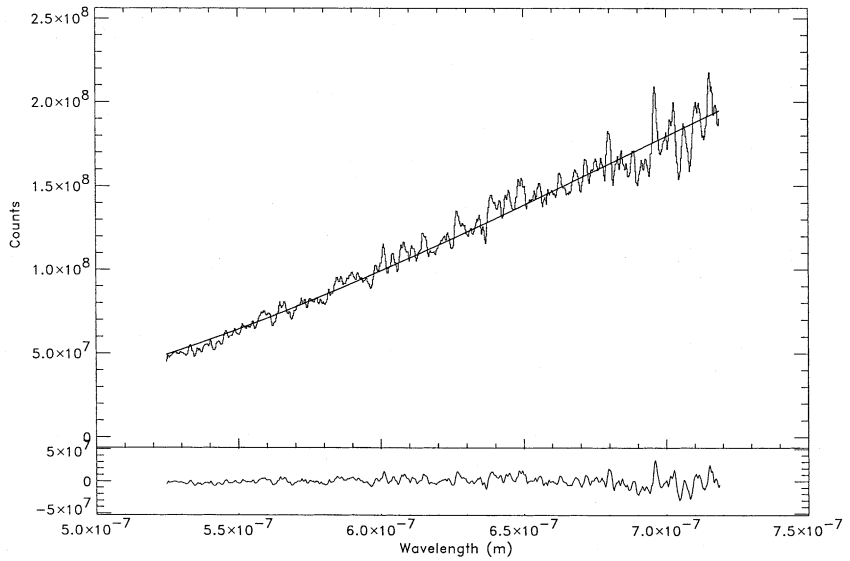

Fig. 2. Example fit of the Planck function to emission spectra ($T = 2512$ K), corrected for system response, from a heated area of a sample with the multimode Nd-YAG laser. (The visible portion of the thermal emission from approximately 525 to 720 nm was used for the Planck grey-body fit for temperature and emissivity [20].)

action) during melting and cooling. In such a way, the quenched melts usually had an adequate surface for analysis. Compositions of the experimental products were analysed on a JEOL JSM-840A scanning electron microscope in the Department of Earth Sciences, University of Oxford, which is equipped with an Oxford Instruments Isis 300 energy-dispersive analytical system (the electron beam is less than 1 μm, with a spatial resolution therefore near 1 μm), and was used for both image acquisition and chemical analysis. The accelerating voltage used was 20 kV, with a beam current of 6 nA. Fe, Ni and Co metals, orthoclase, jadeite, wollastonite, periclase and corundum were employed as standards, as described elsewhere for other work [23]. The spectrometer gain and beam current were checked every 2 h against a Co metal standard. The normal live counting time for an energy spectrum energy was 100 s.

3. Results

The experimental conditions and the resulting exchange partition coefficients are presented in Table 2a,b for Ni- and Co-bearing materials, respectively. The run products contained essentially two phases: the silicate and the Fe-rich alloy phases, as shown in Fig. 3. In all our experiments we found that the silicate phase is amorphous in the range of pressure investigated and we did not observe any crystalline phase after quenching samples from high pressure and high temperature, as indicated by the Raman spectra of these samples. The coefficients of partitioning of Ni and Co determined here are, therefore, coefficients representing liquid–liquid exchange between silicate and metal phases. It was necessary in some instances to eliminate a few anomalously high analyses with roughly 100 wt% of metal-rich phases (either Ni, Co or Fe) that were taken as indication that the starting grains did not form a well-mixed alloy and react with the surrounding silicate. Analyses of the silicate phase that were far from the nominal composition of the starting material were also rejected. As we used unpolished samples the chemical analysis of the silicate phase led to poor microprobe totals (between 94 and 104%). We normalised all the analyses to 100%. Such a procedure does not affect the data presented in this work, especially the exchange partitioning co-

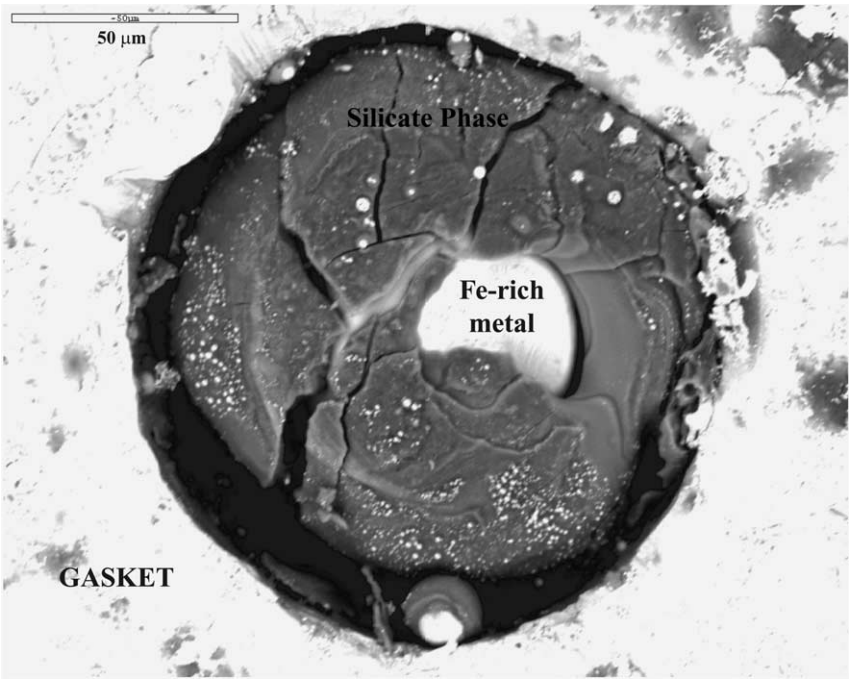

Fig. 3. Backscattered-electron image of one recovered sample from 22.4 GPa and 2500 K. A scale bar is shown at the top left corner. To avoid any contamination of the metal by silicate and vice versa, the area of the silicate analysed was free from metal inclusions (bright spots in the lower part of the figure) and the metal area analysed was the larger spot (centre).

efficients of Ni and Co, which represent the ratios Ni/Fe and Co/Fe in both silicate and metal. The most important criterion during analysis was that the analytical compositions presented are statistically representative of the products after experiments. Further, analysed compositions of silicate and metal phases were consistently close to the bulk starting materials. As shown in Fig. 3 (sample recovered from 22.4 GPa and 2500 K), the size of the quenched silicate phase is about 50 μm, whereas that of the metallic phase is about 20 μm. These sizes permit us to do more than 15 analyses on the silicate phase and about 10 on the Fe alloy. The reported analyses in Table 2a,b are thus the average of several analyses made for the same phase. The silicate phase was analysed for SiO_2, Al_2O_3, FeO, MgO, CaO and NiO or CoO (oxygen is given by stoichiometry). For iron-rich alloys, we limited our results of analyses to Fe, Ni or Co; this is essentially due to the low concentrations (usually within two standard deviations, e.g. near the detection limit) of O, Al, Si, Mg and Ca in our experiments.

For pressures lower than 25 GPa, most samples obtained after heating were similar to that of Fig. 3, although occasionally we observed that the metallic phases were too small to be analysed by electron probe. For pressures higher than 25 GPa, the standard hard stainless-steel gasket thickness was too low and made homogeneous laser heating more difficult because a large portion of the heat produced in the sample by the laser beam was conducted away through the diamond anvils. To increase the thickness of the gasket at these pressures, we used a Re gasket, which increased the thickness at 40 GPa to around 50 μm with 500 μm diamond culets. This thickness ensured we had sufficient material for segregation and analysis in the partitioning experiments.

For high-pressure, high-temperature experiments in the LHDAC, an obvious key factor in the quality of the partitioning experiments is the attainment of equilibrium. The good agreement between the partitioning coefficients determined from DAC experiments and those calculated from the multi-anvil experiments provides the

strongest evidence for the attainment of the equilibrium during the LHDAC experiments (cf. Fig. 3). Further, as the Ni, Co and Fe were added as metal powders dispersed randomly in the starting material, the physical segregation observed in our samples after experiments suggests that the partition coefficients are representative of true equilibrium conditions and not to an artefact of the experiments. In our experiments, the texture of the samples after laser heating appeared determined by surface tension and indicated that the whole sample was melted. At these pressures, the diffusion coefficients for most elements in the liquid are in the range of 10^{-11}–10^{-9} m^2/s in the 1800–2800 K temperature range [24,25]. For the same composition as our starting materials, Thibault and Walter [15] showed that equilibrium partitioning at 5 GPa and above 2300 K for Ni, Co and Fe is accomplished in less than 5 s. Similar studies with MgO capsules showed that at 9 GPa and 2500 K, 2 min is sufficient for Ni and Co to equilibrate between liquid metal and solid magnesiowüstite [26]. Assuming an average of the diffusion coefficient of 10^{-10} m^2/s, the characteristic length ($\lambda = 2\sqrt{Dt}$ where D is the diffusion coefficient and t is time) in a 10–15 min experiment is about 500 μm. This characteristic length is much larger than the run product dimension. Indirect support for the attainment of equilibrium in the LHDAC for partitioning experiments is also shown by the homogeneity of compositions of the two major immiscible liquids.

It is well known that metal–silicate partitioning of siderophile elements is a function of the oxygen fugacity, fO_2 [12,27,28]. It is therefore important to estimate the oxygen fugacity, calculated from the compositions of the run products, of the quenched silicate and metal liquids relative to the iron–wüstite (IW) buffer. In theory, and in high-pressure and high-temperature experiments for iron-bearing compositions, the oxygen fugacity with respect to IW can be calculated based on the Fe and FeO contents of the metal and silicate liquids, respectively, following the relation [29]:

$$\log fO_2(\Delta IW) = 2\log(X^{sil}_{FeO}/X^{met}_{Fe}) \quad (1)$$

where X^{sil}_{FeO} and X^{met}_{Fe} represent the molar fractions of FeO in the silicate liquid and Fe in the metal phase, respectively. This relation assumes ideal behaviour at the high-pressure and high-temperature conditions of the experiments, an assumption that is likely to be valid at higher temperatures especially if liquid–liquid exchange is involved. Using Eq. 1 and data in Table 2a,b, we found that oxygen fugacity in our experiments ranged from 2.1 to 2.3 log units below the IW buffer.

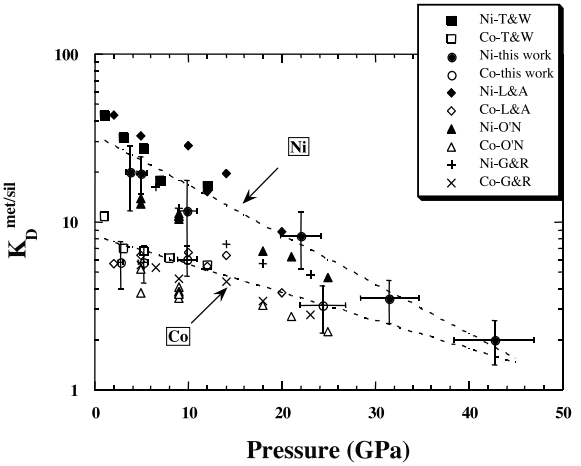

Fig. 4. Exchange coefficients versus pressure. Ni-T&W, Co-T&W are exchange coefficient data from Thibault and Walter [17] for Ni and Co, respectively, Ni-L&A, Co-L&A from Li and Agee [11], Ni-O'N, Co-O'N from O'Neill et al. [36], Ni-G&R, Co-G&R from Gessmann and Rubie [37]. The dashed lines are least-squares fits of the form $\log K_{met/sil} = aP+b$, where a and b are constants (see text). For Ni, $a = 1.51 \pm 0.04$ and $b = -0.027 \pm 0.002$. For Co, $a = 0.92 \pm 0.04$ and $b = -0.017 \pm 0.004$.

In Fig. 4 we plot the exchange partition coefficients determined in this work up to 42 GPa. These coefficients are calculated from the following equation:

$$K_{met/sil} = (X^{met}_M/X^{sil}_{MO})\,(X^{sil}_{FeO}/X^{met}_{Fe}) \quad (2)$$

where X represents mole fraction, X^{met}_M is the mole fraction of M = Ni or Co in metal and X^{sil}_{MO} is the mole fraction of MO = NiO or CoO in silicate. Eq. 2 follows the analysis of O'Neill [30]. An advantage of treating the elemental partitioning as an exchange reaction is that, at constant pressure and temperature, the partition coefficient is constant at varying oxygen fugacity, since Fe, Ni and Co occur only in divalent state in silicates under

relevant conditions [30]. Indeed, on the basis of both 1-atm and high-pressure experiments, Fe, Ni and Co have been shown to be divalent cations in silicate melts over a wide range of oxygen fugacity [17,27,31–35].

As shown in Fig. 4, the coefficients $K_{met/sil}$ for Ni and Co decrease with increasing pressure. This decrease must mainly be due to applied pressure because the temperature remained approximately constant at 2500 ± 200 K and the oxygen fugacity remained around two orders of magnitude lower than the IW buffer. The decrease in $K_{met/sil}$ for Ni is much more pronounced than for Co. In the range 1–42 GPa, $K_{met/sil}$ for Ni decreases more than 25 times, from around 43 ± 4 at 1 GPa [17] to 2.5 ± 0.8 at 42 GPa, whereas for Co, $K_{met/sil}$ decreases by more than three times, from around 11.4 ± 0.7 at 1 GPa [17] to 3.2 ± 1 at 24.4 GPa. A well-known explanation of this behaviour is that both Ni and Co become less siderophile with increasing pressure.

The uncertainties on $K_{met/sil}$ given above were determined assuming that the contribution of small differences in pressure, temperature and oxygen fugacity were negligible. The error in $K_{met/sil}$ is assumed to be a result of uncertainties in the chemical analyses of Fe, Ni and Co present in the silicate and metal phases only. Because of the very low Ni and Co contents in the silicate phase, the measured values of $K_{met/sil}$ for Ni and Co are subject to large uncertainties. For example, the average content of Ni and Co in silicate phase is 0.5 wt% if the standard deviation in this value is in the range of 0.1–0.2 (which is considered as the uncertainty in the content of Ni or Co), the uncertainties in $K_{met/sil}$ are in the range 15–30%. In Table 2a,b we report the $K_{met/sil}$ coefficients, as well as the uncertainties on these coefficients obtained from standard error calculations. The uncertainties in $K_{met/sil}$ coefficients ranged from 18% to 34% of the calculated values.

4. Discussion

The main aim of the present experiments was to first reproduce the partitioning results of multi-anvil devices in a LHDAC and then to extend the uppermost pressure limit. Comparison of the present experimental data with those of Thibault and Walter [17] determined from multi-anvil experiments up to 12 GPa for similar starting compositions, those of Li and Agee [11,12] up to 25 GPa for some sulphur-bearing compositions, those of O'Neill et al. [36] and Gessmann and Rubie [37] up to 25 GPa for iron-rich metal in equilibrium with magnesiowüstite, shows good agreement between the various exchange partition coefficients obtained in all these studies (Fig. 4). The agreement suggests conditions in LHDAC experiments can be made to approach those of multi-anvil experiments in the pressure range we have studied. The partitioning of different elements between an iron-rich alloy and silicate melts can now be performed at pressures appropriate to a major part of the Earth's lower mantle. The close agreement among the various experimental results also suggests that small variations in silicate composition appear to have a small effect on the partitioning of Ni and Co between silicate or oxide melts and Fe-rich metals. In addition, the agreement shows once more the similarities between metal/silicate and metal/oxide distribution coefficients for Ni and Co [11,12,36–39]. The compilation of Walter et al. [6] of partitioning exchange coefficients $K_{met/sil}$ as a function of pressure for Ni and Co between different peridotitic compositions and iron-rich metal liquids with variable S and C contents also shows a similar order of magnitude and behaviour of these coefficients up to 26 GPa. This compilation also supports the fact that the $K_{met/sil}$ coefficients appear little influenced by variable FeO and MgO in silicate melts or by the Fe or S contents of the metal phases [11,12,32]. The partitioning exchange coefficients of Ni and Co shown in Fig. 4 were obtained over the range 2073–2773 K and are plotted without temperature correction. From the overall agreement between studies, the effect of temperature on Ni and Co partitioning appears small [26,36].

The experimental data plotted in Fig. 4 show that the coefficients $K_{met/sil}$ for Ni and Co determined for higher pressures, above 25 GPa, follow the same trend as at lower pressures, and at constant temperature and oxygen fugacity these coef-

ficients can be fit by linear equations of the form $\log K_{met/sil} = aP+b$, where a and b are constants determined from a least-squares fit of the combined data of Thibault and Walter [17] and the data from this work (cf. Fig. 4), which are strictly of the same starting composition.

The results can be directly applied to the issue of the siderophile element anomaly and the composition of the Earth's mantle. Ringwood [1] first recognised the apparent disequilibrium, which cannot be explained by metal/silicate segregation at low pressures [5,40]. There are several mechanisms to explain this anomaly, such as heteregeneous accretion models [4,41], inefficient core formation [9], or equilibration at high pressure and high temperature between iron-rich metal and liquid silicates at the base of a magma ocean [11,12,37]. Our experimental data are applicable to high-pressure and high-temperature homogeneous accretion (HA) models, because all our experiments are equilibrium experiments between metal and silicate liquids with a constant bulk silicate composition. Within the uncertainties on the partitioning coefficients, the ratio (D_{Ni}/D_{Co}) reaches 1.1 in the range 35–45 GPa and is the value required in mass-balance calculations for the whole Earth that demonstrate that the upper mantle's near-chondritic Ni/Co ratio can be produced if D_{Ni} and D_{Co} are around 27 and 24, respectively [40,42]. The range 35–45 GPa obtained from our experimental data is within depth-range estimates for the magma ocean required by most Ni and Co partition studies which argue for an equilibrium signature in the mantle set by liquid silicate and liquid metal.

The combination of our data and those of Thibault and Walter [17], as well as work by Li and Agee [11,12], O'Neill et al. [36], and Gessmann and Rubie [37], suggests a magma ocean would have extended well into the top of the Earth's lower mantle (pressures range from 28 to 45 GPa) in the early Earth under a HA scenario. As the depths required for Ni and Co equilibration increase, so will the likely temperatures required to produce homogeneous melts at the higher pressures. Our results would then be consistent with the suggestion by Gessman and Rubie [37] that abundances of V, Cr and Mn in the mantle are better explained by high temperatures rather than a pressure effect, as long as Ni and Co partitioning remains less temperature-sensitive. The actual effective depth range would be strongly dependent on the kinetics of metal–silicate equilibrium. Rubie et al. [43] have shown that magma-ocean apparent depths will depend upon whether metal equilibrates as droplets or as a layer. They conclude that the concentrations of moderately siderophile elements (e.g. Ni, Co) in the mantle are indeed likely the result of chemical interaction between settling droplets of metal and silicate liquid in a magma ocean, rather than between a segregated layer of liquid silicate overlying liquid metal at the base of the magma ocean.

Holzheid et al. [44] suggested that the observed abundances of Pd and Pt in the upper mantle cannot be explained by the partitioning of paladium and platinum between metal and silicate phases in a HA model. They suggested they are best explained by a late veneer of chondritic material entering the upper mantle after the dominant core formation process. However, Holzheid et al.'s study was limited to pressures below 16 GPa and low temperatures and may not provide the final answer for these highly siderophile elements – Pd and Pt could yet be less siderophile at deeper magma-ocean conditions. It is clear that further partitioning experiments, with both moderately or highly siderophile elements at deep magma-ocean conditions are needed in order to establish a 'unique' mechanism able to explain the whole pattern of siderophile element abundances in the Earth's mantle. Careful studies with the LHDAC may, for the first time, provide access to partitioning data at these extreme conditions.

Acknowledgements

We thank N. Charnley for his help with the SEM analysis. Thorough reviews by H.St.C. O'Neill, K. Righter and D.C. Rubie led to significant improvement of this paper. M.A.B. acknowledges the support of a Marie Curie EU Fellowship (Contract No. HPMF-CT-1999-00329). The experiments were supported in part by NERC Grant GR3/10912 to A.P.J. We thank A.K.

Kleppe for her help during the Raman spectra acquisition, and P. Richet for laboratory support for glass synthesis.*[BW]*

References

[1] A.E. Ringwood, Chemical evolution of the terrestrial planets, Geochim. Cosmochim. Acta 30 (1966) 41–104.
[2] R. Brett, Chemical equilibrium of the Earth's core and upper mantle, Geochim. Cosmochim. Acta 48 (1984) 1183–1188.
[3] H.E. Newsom, K.W.W. Sims, Core formation during early accretion of the Earth, Science 252 (1991) 926–933.
[4] H.St.C. O'Neill, The origin of the Moon and the early history of the Earth-chemical model. Part 2: the Earth, Geochim. Cosmochim. Acta 55 (1991) 1159–1172.
[5] H. Palme, H.St.C. O'Neill, Formation of the Earth's core, Geochim. Cosmochim. Acta 60 (1996) 1106–1108.
[6] M.J. Walter, H.E. Newsom, W. Ertel, A. Holzheid, Siderophile elements in the Earth and Moon: Metal/silicate partitioning and implications for core formation, in: R.M. Canup, K. Righter (Eds.), Origin of the Earth and Moon, The University of Arizona Press, 2000, pp. 265–289.
[7] H. Wänke, Constitution of terrestrial planets, Philos. Trans. R. Soc. Lond. A 303 (1981) 287–302.
[8] R.J. Arculus, J.W. Delano, Siderophile element abundances in the upper mantle: evidence for a sulfide signature and equilibrium with the core, Geochim. Cosmochim. Acta 45 (1981) 1331–1343.
[9] J.H. Jones, M.J. Drake, Geochemical constraints on core formation in the Earth, Nature 322 (1986) 221–228.
[10] K. Righter, M. Drake, Metal-silicate equilibrium in a homogeneously accreting Earth: new results for Re, Earth Planet. Sci. Lett. 146 (1997) 541–553.
[11] J. Li, C.B. Agee, Geochemistry of mantle-core differentiation at high pressure, Nature 381 (1996) 686–689.
[12] J. Li, C.B. Agee, The effect of pressure, temperature, oxygen fugacity and composition on partitioning of nickel and cobalt between liquid Fe-Ni-S alloy and liquid silicate: Implications for the Earth's core formation, Geochim. Cosmochim. Acta 65 (2001) 1821–1832.
[13] H.E. Newsom, Accretion and core formation in the Earth: evidence from siderophile elements, in: H.E. Newson, J.H. Jones (Eds.), Origin of the Earth, Oxford University Press, New York, 1990, pp. 273–288.
[14] L. Grossman, Condensation in the primitive solar nebula, Geochim. Cosmochim. Acta 36 (1972) 597–619.
[15] H.St.C. O'Neill, H. Palme, Composition of the silicate Earth: Implications for accretion and core formation, in: I. Jackson (Ed.), The Earth's Mantle, Composition, Structure, and Evolution, Cambridge University Press, 1998, pp. 3–126.
[16] V.J. Hillgren, M.J. Drake, D.C. Rubie, High-pressure and high-temperature experiments on core-mantle segregation in the accreting Earth, Science 264 (1994) 1442–1445.
[17] Y. Thibault, M.J. Walter, The influence of pressure and temperature on the metal-silicate partition coefficients of nickel and cobalt in a model C1 chondrite and implications for metal segregation in a deep magma ocean, Geochim. Cosmochim. Acta 59 (1995) 991–1002.
[18] A.P. Jephcoat, H.K. Mao, P.M. Bell, Operation of the Megabar Diamond-Anvil Cell, in: Hydrothermal Experimental Techniques, Wiley-Interscience, New York, 1987, pp. 469–506.
[19] H.K. Mao, P.M. Bell, J.W. Shaner, D.J. Steinberg, Specific volume measurements of Cu, Mo, Pd and Ag and calibration of the ruby R1 fluorescence pressure gauge from 0.06 to 1 Mbar, J. Appl. Phys. 49 (1976) 3276–3283.
[20] A.P. Jephcoat, S.P. Besedin, Temperature measurement and melting determination in the laser-heated diamond-anvil cell, Philos. Trans. R. Soc. Lond. A 354 (1996) 1333–1360.
[21] G.H. Miller, E.M. Stolper, T.J. Ahrens, The equation of state of a molten komatiite. 2. Application to komatiite petrogenesis and the hadean mantle, J. Geophys. Res. 96 (1991) 11849–11864.
[22] D. Andrault et al., Thermal pressure in the laser-heated diamond-anvil cell: An X-ray diffraction study, Eur. J. Mineral. 10 (1998) 931–940.
[23] D. Waters, N. Charnley, Ti substitution in metamorphic biotite, Am. Mineral. 87 (2002) 383–396.
[24] D. Walker, C.B. Agee, Partitioning 'equilibrium', temperature gradients, and constraints on Earth differentiation, Earth Planet. Sci. Lett. 96 (1989) 49–60.
[25] J.E. Reid, B.T. Poe, D.C. Rubie, N. Zotov, M. Wiedenbeck, The self-diffusion of silicon and oxygen in diopside ($CaMgSi_2O_6$) liquid up to 15 GPa, Chem. Geol. 174 (2001) 77–86.
[26] C.K. Gessmann, D.C. Rubie, The effect of temperature on the partitioning of nickel, cobalt, manganese, chromium, and vanadium at 9 GPa and constraints on formation of the Earth's core, Geochim. Cosmochim. Acta 62 (1998) 867–882.
[27] W. Schmitt, H. Palme, H. Wänke, Experimental determination of metal/silicate partition coefficients for P, Co, Ni, Cu, Ga, Ge, Mo and W and some implications for the early evolution of the Earth, Geochim. Cosmochim. Acta 53 (1989) 173–185.
[28] C.K. Gessmann, D.C. Rubie, C.A. McCammon, Oxygen fugacity dependence of Ni, Co, Mn, Cr, V, and Si partitioning between liquid metal and magnesiowustite at 9-18 GPa and 2200 C, Geochim. Cosmochim. Acta 63 (1999) 1853–1863.
[29] M.J. Drake, H.E. Newsom, C.J. Capobianco, V, Cr and Mn in the Earth, Moon, EPB, and SPB and the origin of the Moon: Experimental studies, Geochim. Cosmochim. Acta 53 (1989) 2101–2111.
[30] H.St.C. O'Neill, Siderophile elements and the Earth's formation, Science 257 (1992) 1281–1285.

[31] C.J. Capobianco, A.A. Amelin, Metal/silicate partitioning of nickel and cobalt: the influence of temperature and oxygen fugacity, Geochim. Cosmochim. Acta 58 (1994) 125–140.
[32] A. Holzheid, H. Palme, The influence of FeO on the solubilities of Co and Ni in silicate melts, Geochim. Cosmochim. Acta 60 (1996) 1181–1193.
[33] A. Holzheid, A. Borisov, H. Palme, The effect of oxygen fugacity and temperature on solubilities of nickel, cobalt, and molybdenum in silicate melts, Geochim. Cosmochim. Acta 58 (1994) 1975–1981.
[34] D.B. Dingwell, H.S.C. O'Neill, W. Ertel, B. Spettel, The solubility and oxidation state of Ni in silicate melt at low oxygen fugacity: results using a mechanically assisted equilibrium technique, Geochim. Cosmochim. Acta 58 (1994) 1967–1974.
[35] V.J. Hillgren, M.J. Drake, D.C. Rubie, High pressure and high temperature metal-silicate partitioning of siderophile elements: The importance of silicate liquid composition, Geochim. Cosmochim. Acta 60 (1996) 2257–2263.
[36] H.St.C. O'Neill, D. Canil, D.C. Rubie, Oxide-metal equilibria to 2500°C and 25 GPa: Implications for core formation and the light component in the Earth's core, J. Geophys. Res. 103 (1998) 12239–12260.
[37] C.K. Gessmann, D.C. Rubie, The origin of the depletions of V, Cr and Mn in the mantles of the Earth and Moon, Earth Planet. Sci. Lett. 184 (2000) 95–107.
[38] E. Ohtani, H. Yurimoto, Element partitioning between metallic liquid, magnesiowustite, and silicate liquid at 20 GPa and 2500°C: A secondary ion mass spectrometric study, Geophys. Res. Lett. 23 (1996) 1993–1996.
[39] E. Ito, T. Katsura, T. Suzuki, Metal/silicate partitioning of Mn, Co, and Ni at high-pressures and high-temperatures and implications for core formation in a deep magma ocean, in: M.H. Manghnani, T. Yagi (Eds.), Properties of Earth and Planetary Materials at High Pressure and Temperature, Am. Geophys. Union, Washington, DC, 1998, pp. 215–225.
[40] H.St.C. O'Neill, H. Palme, Composition of the silicate Earth: Implications for accretion and core formation, in: The Earth's Mantle: Structure, Composition and Evolution, Cambridge University Press, New York, 1997, pp. 3–125.
[41] H. Wänke, G. Dreibus, E. Jagoutz, Mantle chemistry and accretion history of the Earth, in: A. Kröner et al. (Eds.), Archaean Geochemistry: The Origin and Evolution of the Archaean Continental Crust, Springer, Berlin, 1984, pp. 1–24.
[42] M.F. McDonough, S.-s Sun, The composition of the Earth, Chem. Geol. 120 (1995) 223–253.
[43] D.C. Rubie, H.J. Melosh, J.E. Reid, C. Liebske, K. Righter, Mechanisms of metal-silicate equilibration in the terrestrial magma ocean, Earth Planet. Sci. Lett. 205 (2003) 239–255.
[44] A. Holzheid, P. Sylvester, H.St.C. O'Neill, D.C. Rubie, H. Palme, Evidence for a late chondritic veneer in the Earth's mantle from high-pressure partitioning of palladium and platinum, Nature 406 (2000) 396–399.